OXFORD

SOT | Society of Toxicology
www.toxsci.oxfordjournals.org

TOXICOLOGICAL SCIENCES, 151(1), 2016, 44–56

doi: 10.1093/toxsci/kfw021
Advance Access Publication Date: January 27, 2016
Research Article

Loss of Mrp1 Potentiates Doxorubicin-Induced Cytotoxicity in Neonatal Mouse Cardiomyocytes and Cardiac Fibroblasts

Wei Zhang,* Daret St Clair,* Allan Butterfield,† and Mary Vore*,[1]

*Department of Toxicology and Cancer Biology, College of Medicine, University of Kentucky, Lexington, Kentucky 40536; and †Department of Chemistry, University of Kentucky, Lexington, Kentucky 40506

[1]To whom correspondence should be addressed at Department of Toxicology and Cancer Biology, University of Kentucky, 306 Health Sciences Research Building, Lexington, KY 40536. Fax: (859) 323-1059. E-mail: maryv@email.uky.edu.

ABSTRACT

Doxorubicin (DOX) induces dose-dependent cardiotoxicity in part due to its ability to induce oxidative stress. We showed that loss of multidrug resistance-associated protein 1 (Abcc1/Mrp1) potentiates DOX-induced cardiac dysfunction in mice *in vivo*. Here, we characterized DOX toxicity in cultured cardiomyocytes (CM) and cardiac fibroblasts (CF) derived from C57BL wild type (WT) and Mrp1 null (Mrp1−/−) neonatal mice. CM accumulated more intracellular DOX relative to CF but this accumulation did not differ between genotypes. Following DOX (0.3–4 μM), Mrp1−/− CM, and CF, especially CM, showed a greater decrease in viability and increased apoptosis and DNA damage, demonstrated by higher caspase 3 cleavage, poly (ADP-ribose) polymerase 1 (PARP) cleavage and phosphorylated histone H2AX (γH2AX) levels versus WT cells. Saline- and DOX-treated Mrp1−/− cells had significantly higher intracellular GSH and GSSG compared with WT cells ($P < .05$), but the redox potential (*Eh*) of the GSH/GSSG pool did not differ between genotypes in CM and CF, indicating that Mrp1−/− cells maintain this major redox couple. DOX increased expression of the rate-limiting GSH synthesis enzyme glutamate-cysteine ligase catalytic (GCLc) and regulatory subunits (GCLm) to a significantly greater extent in Mrp1−/− versus WT cells, suggesting adaptive responses to oxidative stress in Mrp1−/− cells that were inadequate to afford protection. Expression of extracellular superoxide dismutase (ECSOD/SOD3) was lower ($P < .05$) in Mrp1−/− versus WT CM treated with saline (62% ± 8% of WT) or DOX (43% ± 12% of WT). Thus, Mrp1 protects CM in particular and CF against DOX-induced toxicity, potentially by regulating extracellular redox states.

Key words: Mrp1; doxorubicin; glutathione; glutathione disulfide; ECSOD

Doxorubicin (DOX), an anthracycline, is a highly effective and commonly used chemotherapy drug for a variety of malignant tumors. However, cardiac toxicity is a serious adverse reaction associated with the administration of DOX (Octavia *et al.*, 2012). Cancer patients treated with DOX have a 2.5-fold higher incidence of cardiomyopathy than untreated patients (Doyle *et al.*, 2005). Therefore, identifying the gene(s) involved in normal hearts' defense against this toxicity and understanding the mechanisms will help identify potential approaches to alleviate the clinical cardiotoxicity of chemotherapy.

Multidrug resistance-associated protein 1 (MRP1/ABCC1), a member of the ATP-binding cassette (ABC) transporter protein superfamily, is ubiquitously expressed, especially in heart, skin, lung, brain capillary endothelial cells, and the small intestine (Flens *et al.*, 1996; Nies *et al.*, 2004). It mediates efflux of glutathione (GSH), glutathione disulfide (GSSG), as well as GS-, glucoronate-, and sulfate-conjugates (Cole, 2014a,b; Cole and Deeley, 1998; Leslie *et al.*, 2001). Although Mrp1−/− mice have normal fertility and viability, their ability to transport some endobiotics and xenobiotics is compromised (Krohn *et al.*, 2011; Li *et al.*, 2005; Wijnholds *et al.*, 1997). Because Mrp1 plays an important

role in the efflux of endobiotics and xenobiotics and their conjugates from various organs, it can protect tissues from toxicity. More importantly, clinical studies show that genetic variants of MRP1 are associated with increased susceptibility to cardiotoxicity in cancer patients treated with anthracyclines, including DOX (Semsei *et al.*, 2012; Visscher *et al.*, 2012; Wojnowski *et al.*, 2005). Our *in vivo* studies demonstrate that loss of Mrp1 potentiates DOX-induced cardiotoxicity in mice, with Mrp1−/− mice exhibiting more nuclear injury after a single acute dose (15 mg/kg) and greater apoptosis and cardiac dysfunction following chronic DOX treatment (Deng *et al.*, 2015; Zhang *et al.*, 2015). It is important to point out that although Mrp1 is highly conserved between human and rodents, with 88% sequence homology, the human isoform (MRP1) is able to transport DOX, whereas murine Mrp1 has a negligible ability to transport this anthracycline antibiotic (Stride *et al.*, 1997). Therefore, any effects of Mrp1 in mouse studies cannot be attributed to efflux of DOX.

Cardiomyocytes (CM) and cardiac fibroblasts (CF) form the 2 largest cell populations in heart, and other cell types, such as endothelial or vascular smooth muscle cells, represent comparatively small populations. CM are the primary cells that make up the atria and ventricles of the heart, and account for more than 50% of the total cell number. CM must be able to shorten and lengthen properly to maintain normal cardiac structure and function and because they are continuously contracting, utilize large amounts of ATP generated by mitochondria. Significant evidence indicates that death of CM by apoptosis and necrosis is an important mechanism of DOX-induced cardiomyopathy (Octavia *et al.*, 2012; Zhang *et al.*, 2009). CF are the most abundant nonmyocytes within the heart and are found throughout cardiac tissue, surrounding CM and bridging "the voids" between myocardial tissue layers. CF contribute to cardiac development, myocardial structure, cell signaling, and electromechanical function in healthy myocardium (Camelliti *et al.*, 2005). Beyond its very important roles in maintaining normal myocardial function, CF also contribute to adverse cardiac remodeling during pathological conditions, such as hypertension, myocardial infarction, and heart failure (Shi *et al.*, 2011; Souders *et al.*, 2009), and are involved in arrhythmia initiation and maintenance by affecting electrical propagation (Kamkin *et al.*, 2005).

Here, to extend the bases of Mrp1's cardiac protective role to a cellular level, and identify the specific functions of Mrp1 in different cell types in heart, we further investigated the role of Mrp1 in DOX toxicity in neonatal mouse CM and CF. Our data demonstrate that DOX increased Mrp1 expression in neonatal mouse CM and CF cultures, and cells derived from Mrp1−/− mice were more sensitive to DOX toxicity despite higher basal levels of intracellular GSH. Importantly, Mrp1−/− CM showed lower extracellular superoxide dismutase (ECSOD) expression than wild type (WT) CM, which likely potentiates DOX toxicity in Mrp1−/− CM. These data demonstrate that Mrp1 protects both CM and CF against DOX toxicity and provides novel insights into the role of Mrp1 in redox status regulation.

MATERIALS AND METHODS

Cell culture

C57BL/6J (WT) mice and Mrp1-disrupted C57BL/6 (Mrp1−/−) mice were backcrossed for more than 10 generations, bred in-house and maintained in the Division of Laboratory Animal Resources. Mrp1−/− mice are available at The Jackson Laboratory Repository (JAX Stock No. 028129). All experiments complied with the requirements of the Institutional Animal Care and Use Committee of the University of Kentucky (Lexington, Kentucky). Primary CM and CF were obtained from Mrp1−/− neonatal mice and their WT littermates at 1–3 days of age based on published methods with minor modification (Fu *et al.*, 2010; Yin *et al.*, 2014). Mice were sacrificed by cervical dislocation, hearts removed aseptically with the ventricles only retained and maintained in cold Hanks' balanced salt solution (HBSS) without Ca^{2+} and Mg^{2+}. The ventricles were washed with the same HBSS and minced into small fragments that were subjected to enzymatic digestion with collagenase type 2 (Worthington Biochemical Corp, Lakewood, New Jersey) in HBSS, with serial cycles of agitation. After each cycle, the supernatant (containing the isolated cells) was removed and fetal bovine serum (FBS) added to a final concentration of 10%, the resulting mixture centrifuged for 10 min at 100 × g, and then the cells resuspended in DMEM with 10% FBS (vol/vol), 100 units/ml penicillin, and 100 μg/ml streptomycin (GIBCO, Grand Island, New York). Cells were preplated for 2 h at 37°C, to obtain CM and nonmyocyte cells, predominantly CF. For CM culture, 100 μmol/l bromodeoxyuridine (Sigma Chemical Co) was added during the first 48 h to prevent proliferation of nonmyocytes. CM and CF culture were routinely examined for purity of the preparation by immunofluorescence staining of cardiac-sarcomeric actinin (mouse anti-α-actinin mAb [A7811, Sigma Chemical Co] and Alexa Fluor 594-conjugated goat anti-mouse IgG [A-21125, Life Technologies, Carlsbad, California]) for CM and vimentin (mouse anti-vimentin mAb [sc73259, Santa Cruz Biotechnology] and Alexa Fluor 680-conjugated goat anti-mouse IgG [A-21058, Invitrogen, Carlsbad, California]) for CF (Supplementary Figure 1). CF cultures were used for experiments after 2 passages to eliminate other nonmyocytes. CM purity averaged > 95% and CF purity was almost 100% at the time cells were treated.

Accumulation of DOX in WT and Mrp1−/− CM and CF

Cells were treated with 30 μM DOX for 1 h, washed 3 times with PBS, and incubated with fresh DMEM medium for 0, 2, and 4 h. Finally, cells were washed 3 times with PBS and incubated in acidified (0.75 N HCl) isopropanol and shaken for 30 min at room temperature. The inherent fluorescence associated with the central anthracycline chromophore group of DOX in the supernatant was read using a spectrofluorometer at wavelengths of Ex = 470 nm and Em = 590 nm. Detection of DOX in all samples was in the range of linearity, which extended from 0.08–5 ng/μl. The value of DOX accumulation within the cells was calculated according to the standard curve. Each point represents the mean ± SD ($n = 3$).

Methyl thiazol tetrazolium assay

The cytotoxicity of DOX was determined by the methyl thiazol tetrazolium (MTT) test. WT and Mrp1−/− CM or CF cells were seeded and grown in a 96-well plate at 37°C in a 5% CO_2 saturated atmosphere overnight. To develop a dose-response curve, DOX stock solution (2 mg/ml, Pfizer, New York) was dissolved in culture medium to final concentrations of 0–4 μM, and was incubated with cells in culture for 3 h, after which the media containing DOX was removed. Cells were rinsed once with ×1 PBS, and finally incubated with fresh media for an additional 48 h. The MTT assay was performed according to the manufacturer's instructions (CellTiter 96 Aqueous One Solution Cell Proliferation Assay, Promega, Madison, Wisconsin). The

absorbance at 480 nm was measured for each well by a SpectraMax M5 multidetection reader (Molecular Devices, Sunnyvale, California). The absorbance of untreated control cells was taken as 100% viability and the values of treated cells were calculated as a percentage of control. The data are represented as mean ± SD from 3 independent experiments.

High Performance Liquid Chromatography (HPLC) assay of GSH and GSSG

CM (10^6 cells) or CF (3×10^5 cells) were plated and cultured on 6-well plates overnight, then treated with 0.5 μM DOX (CM) or 1 μM DOX (CF) for 15 min or 3 h. Cells were scraped immediately or following an additional 24 h, and then lysed with RIPA buffer and cell lysate used for GSH derivatization and quantification of GSH and GSSG. The measurement of GSH and GSSG by HPLC was done exactly as described (Deng *et al.*, 2015). The redox potential (*Eh*) of the GSH/GSSG pool was calculated using the estimated cellular GSH and GSSG concentrations and the Nernst equation: $Eh = Eo + (RT/nF)\ \ln([GSSG]/[GSH]^2)$. To estimate cellular concentrations, 1 mg of cell protein was assumed to be associated with 5 μl of cell volume (Mannery *et al.*, 2010). R is the gas constant, T is temperature, *n* is the number of electrons transferred, F is the Faraday constant, and $Eo = -264$ mV at a pH of 7.4.

Immunoblot assay

Protein concentrations were determined using the bicinchoninic acid protein assay (Pierce, Rockford, Illinois). Protein samples were fractionated on a 4%–12% SDS-PAGE gel (EC6038BOX, Life Technologies) and transferred to nitrocellulose (Whatman, Stanford, Maine). The blots were incubated with the primary antibody diluted in TBS/5% nonfat milk/0.1% Tween 20 at 4°C overnight, then washed in TBS/0.1% Tween 20, and subsequently incubated with horseradish peroxidase (HRP)-labeled secondary antibody in TBS/5% nonfat milk/0.1% Tween 20. Chemiluminescence detection was done using Enhanced Chemiluminescence Plus (RPN2236, GE Healthcare, UK). Antibodies were obtained as follows: rat anti-Mrp1 mAb (801-007-c250; Alexis, San Diego, California), rabbit anti-glyceraldehyde-3-phosphate dehydrogenase pAb (sc-25778), and rabbit anti-actin pAb (sc-1616-R) from Santa Cruz Biotechnology; rabbit anti-PARP (poly (ADP-ribose) polymerase 1) pAb (No. 9542), rabbit anti-cleaved caspase 3 pAb (No. 9661), and rabbit anti–phospho-histone H2A.X (γH2A.X) pAb (Ser139) (No. 9718) from Cell Signaling (Beverly, Massachusetts); rabbit anti–glutamate-cysteine ligase catalytic subunit (GCLc) pAb (ab80841) and rabbit anti-glutamate-cysteine ligase regulatory subunit (GCLm) pAb (ab8144) from Abcam (Cambridge, Massachusetts); and anti-rat Ig-HRP, anti-rabbit Ig-HRP, and anti-mouse Ig-HRP from Amersham Biosciences (Piscataway, New Jersey). Rabbit anti-ECSOD pAb was a generous gift from Dr Ladislav Dory, University of North Texas.

RNA extraction and real-time quantitative PCR

Total RNA was isolated from CM and CF using GenElute Mammalian Total RNA Miniprep Kit (RTN350, Sigma-Aldrich, St Louis, Missouri) according to the manufacturer's instructions. RNA concentrations were determined spectrophotometrically with a NanoPhotometer (Implen GmbH, München, Delaware). Equal amounts of total RNA were converted into cDNA with SuperScript III First-Strand Synthesis System for real-time (RT)-PCR (Invitrogen), and the cDNA mixture diluted without purification in sterile ddH_2O and used for qRT-PCR analysis. Expression of specific genes was quantified by qRT-PCR using the LightCycler 480 Real-Time PCR System (Roche Applied Science, Mannheim, Germany). Primers used for qRT-PCR were ordered from Integrated DNA Technologies (Coralville, Iowa); Universal ProbeLibrary probes were obtained from Roche Applied Science. Primers and probes are shown in Table 1.

Statistical analysis

All data are expressed as the mean ± SD for $n = 3$–6 per group, as detailed in the figure legends. In studies comparing 2 groups, statistical analysis was performed with the Student's *t* test. In studies comparing multiple groups to the same control group, statistical analysis was performed with 1-way ANOVA followed by Dunnett's posttest. In studies comparing more than 2 groups, statistical analysis was performed with 1-way ANOVA followed by Newman-Keuls multiple comparison test.

RESULTS

DOX Upregulates Mrp1 Expression in CM and CF

To examine the effect of DOX on expression of Mrp1, CM, and CF were isolated from WT neonatal mouse heart and treated with DOX for 24 h, followed by measurement of Mrp1 expression by RT-PCR and immunoblotting. As shown in Figure 1, Mrp1 was constitutively present in CM and CF. Moreover, DOX treatment significantly increased both Mrp1 mRNA (Figure 1A) and protein expression (Figure 1C) in CM in a concentration-dependent manner. A similar pattern was observed in CF cultures (Figs. 1B and D). The increase in Mrp1 occurred at a lower dose (1 μM) and to a greater extent in CM (approximately 2.5-fold) than in CF, where 1 μM DOX had no effect on Mrp1 expression, and a higher dose (2 μM) increased Mrp1 expression approximately 1.7-fold. These results imply that Mrp1 is involved in the cellular response to DOX.

Effect of Mrp1 on DOX-Induced Cytotoxicity

To characterize the role of Mrp1 in a cell type specific manner, the cytotoxicity of DOX in WT and Mrp1−/− CM and CF was measured using the MTT assay (Figure 2A). After 3 h of DOX treatment following incubation with DOX-free media for another 48 h, 0.3, 1, and 3 μM DOX decreased viability to 64% ± 3% (mean ± SD), 35% ± 3%, and 11% ± 2%, respectively, in Mrp1−/− CM compared with 75% ± 2%, 52% ± 6%, and 25% ± 5% viability in WT ($P < .05$). Similar experiments demonstrated that CF isolated from Mrp1−/− mice also showed enhanced DOX toxicity (Figure 2B), although the concentration of DOX required to decrease viability by approximately 50% was higher in CF (2 μM) versus that in CM (1 μM).

To understand the mechanism of cell death, we also characterized apoptosis-related proteins in WT and Mrp1−/− CM and CF. DOX treatment increased PARP cleavage and caspase 3 cleavage, and these increases were significantly greater in Mrp1−/− versus WT CM (Figure 2C). The increased phosphorylation of H2AX was observed at early time points and continued to increase over time (3, 6, and 12 h after treatment with DOX) (data not shown); γH2AX was significantly higher in Mrp1−/− CM compared with WT CM 24 h after DOX treatment (Figure 2E). Similar results were observed in CF cultures (Figs. 2D and F), although again, CM showed greater DOX-induced injury. Thus, 1 μM DOX caused approximately 3.3-fold greater caspase 3 cleavage in Mrp1−/− versus WT cells, whereas 3 μM DOX

TABLE 1. The Primers Used for Real-Time Quantitative PCR

Genes	Forward Primer (5′–3′)	Reverse Primer (5′–3′)	Universal Probe Library Probe
18s rRNA	gcaattattccccatgaacg	gggacttaatcaacgcaagc	48
GPx1	tttcccgtgcaatcagttc	tcggacgtacttgagggaat	2
GPx3	ggcttcccttccaaccaa	cccacctggtcgaacatact	92
GSTM1	gcagctcatcatgctctgtta	tttctcagggatggtcttcaa	106
GSTM2	agttggccatggtttgctac	agcttcatcttctcagggagac	106
GCLc	ctgcacatctaccacgcagt	gaacatcgcctccattcagt	SYBR green
GCLm	tgactcacaatgacccgaaa	tcaatgtcagggatgctttct	108
HO-1	aggctaagaccgccttcct	tgtgttcctctgtcagcatca	17
Mrp1	tgtgggaaaacacatctttga	ctgtgcgtgaccaagatcc	105
NQO1	agcgttcggtattacgatcc	agtacaatcagggctcttctcg	50
SOD3	ctcttgggagagcctgaca	gccagtagcaagccgtagaa	102

GPx, glutathione peroxidase; GST, glutathione S-transferase; HO-1: heme oxygenase 1; NQO1, NAD(P)H dehydrogenase, quinone 1; GCLc, glutamate-cysteine ligase catalytic subunit; GCLm, glutamate-cysteine ligase regulatory subunit; Mrp1, multidrug resistance-associated protein 1; SOD3, superoxide dismutase 3.

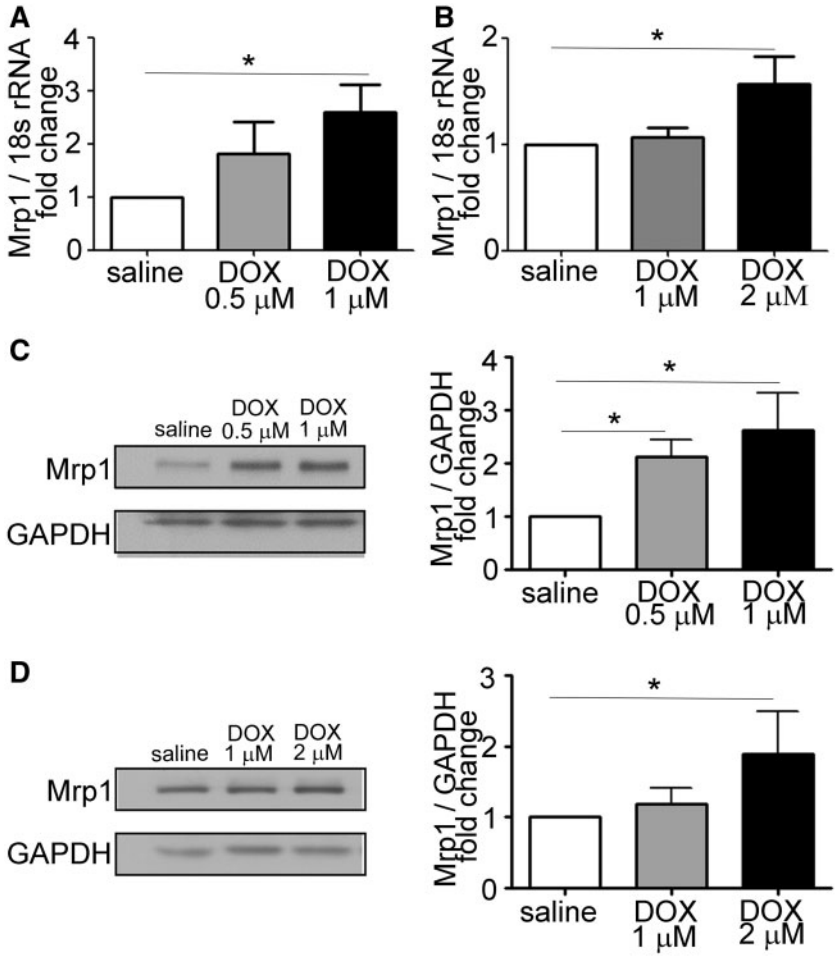

FIG. 1. Doxorubicin (DOX) increases multidrug resistance-associated protein 1 (Mrp1) expression in cardiomyocytes (CM) and cardiac fibroblasts (CF). Quantitative analysis of Mrp1 mRNA and protein expression in CM (A, C) and CF (B, D) 24 h after treatment with saline or varying concentrations of DOX. Immunoblots are representative of 1 of 3 independent experiments. Each bar represents the mean ± SD. (*$P < .05$ by Dunnett's posttest after 1-way ANOVA).

increased caspase 3 cleavage approximately 2.5-fold in Mrp1−/− versus WT cells.

Accumulation of DOX in WT and Mrp1−/− CM and CF

Although no evidence has shown that murine Mrp1 is able to transport DOX, we further examined the intracellular DOX accumulation in WT and Mrp1−/− cells (Figure 3). We did not detect any differences in DOX intracellular retention between genotypes, thus ruling out intracellular DOX accumulation as the cause of the different susceptibility to DOX in WT versus Mrp1−/− cells. These data are also consistent with our *in vivo* mouse studies showing no differences in retention of DOX in the heart at 3, 6, and 24 h after a single intravenous dose of DOX

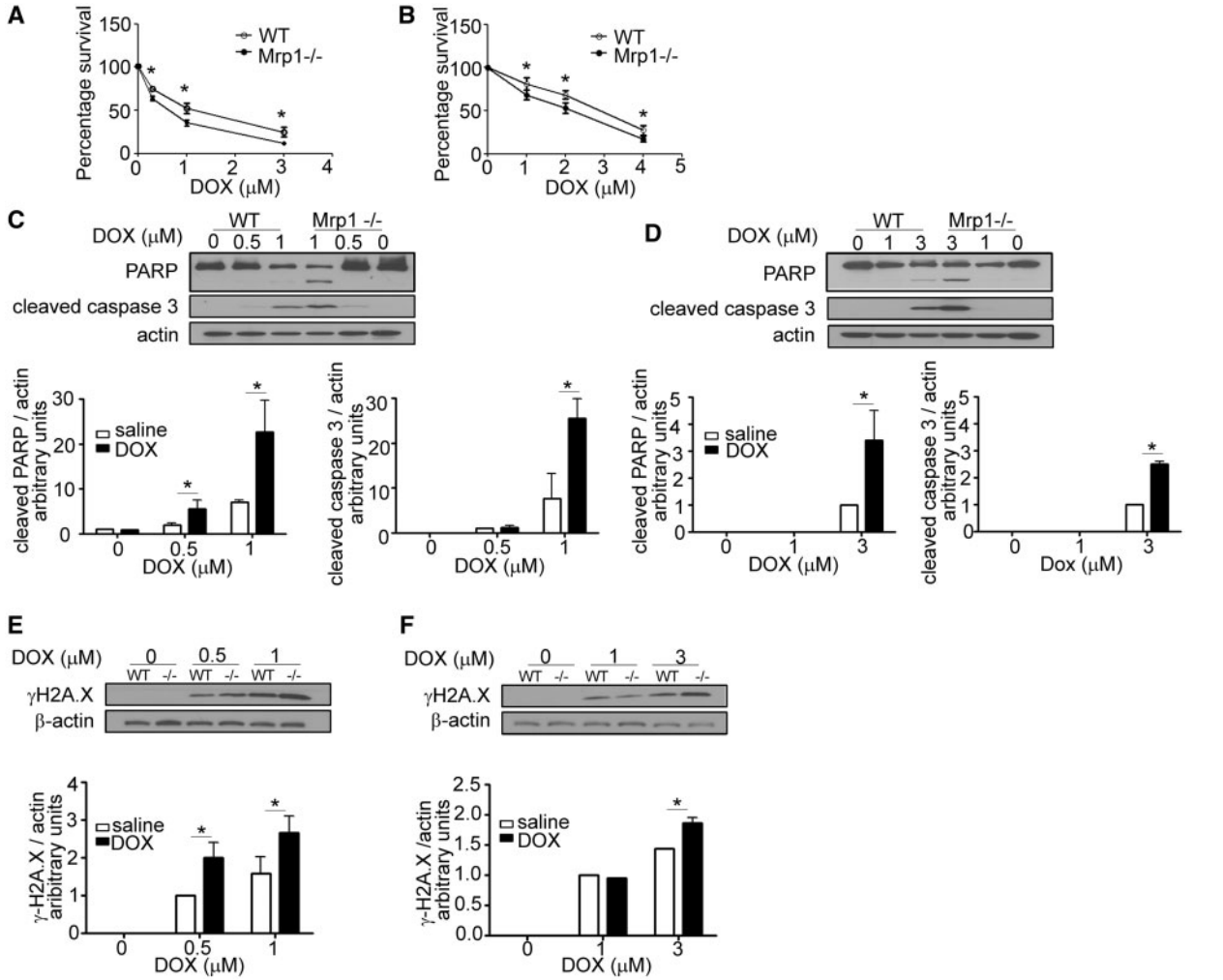

FIG. 2. Effects of DOX on cell viability and DNA damage in wild type (WT) and Mrp1−/− cells. CM (A) and CF (B) were cultured on a 96-well plate for 48 h before treatment with varying concentrations of DOX for 3 h, followed by incubation in fresh medium. Tetrazolium reduction was measured 48 h after DOX removal. Each point represents the mean ± SD from 3 independent experiments (*$P < .05$ by Student's t test). The greater increase of cleaved poly (ADP-ribose) polymerase 1 (PARP), cleaved caspase-3 and γH2A.X in CM (C and E) and CF (D and F) derived from Mrp1−/− mice was detected by immunoblot assays 24 h after 3 h of DOX treatment. The blots are representative of 1 of 3 independent experiments. Each bar represents the mean ± SD. (*$P < .05$ by Newman-Keuls multiple comparison test after 1-way ANOVA).

(15 mg/kg) (Deng *et al.*, 2015). However, the intracellular accumulation of DOX in CM was about twice that in CF, likely due to the higher content of mitochondria in CM versus CF (Barth *et al.*, 1992) and the specific binding of DOX to mitochondrial cardiolipin (Varga *et al.*, 2015).

GSH and GSSG Measurement in CM and CF

As GSH and GSSG are known substrates for Mrp1, we investigated how loss of Mrp1 would alter GSH and GSSG levels in the cell, and therefore disrupt the balance of the GSH/GSSG redox couple. Untreated Mrp1−/− CM and CF had significantly higher GSH and GSSG compared with WT cells (Figure 4), but there was no difference in the GSH/GSSG redox couple between genotypes, consistent with *in vivo* studies in mice (Lorico *et al.*, 1997; Zhang *et al.*, 2015). We further investigated how DOX, a drug known to induce oxidative stress (Chen *et al.*, 2006; Yen *et al.*, 1996), would influence GSH and GSSG. Initial studies examined the time course of the changes in GSH and GSSG in cells over 24 h following DOX treatment, and showed an early decrease in GSH that recovered across time. Subsequent in-depth studies demonstrated that GSH decreased while GSSG increased in both WT and Mrp1−/− CM within 15 min of 0.5 μM DOX, leading to a significant decrease in the GSH/GSSG ratio (Figure 5A). In contrast, in CF, GSH was not decreased while GSSG was modestly but significantly increased following 1 μM DOX in both genotypes so that the GSH/GSSG ratio was not changed in either genotype (Figure 5B). By 24 h after DOX, GSH, GSSG, and the GSH/GSSG ratio had returned to that in saline controls in both CM and CF from WT mice. However, both GSH and GSSG remained significantly increased relative to saline controls in both CM and CF from Mrp1−/− mice 24 h after DOX, resulting in a GSH/GSSG ratio that was the same as saline controls (Figs. 5C and D). As a consequence, the redox potential (Eh) of the GSH/GSSG pool did not differ at 15 min or 24 h between genotypes with either treatment (Figure 5A, Tables 2 and 3).

Expression of Enzymes for GSH Biosynthesis and Recycling

The increase in GSH and GSSG after DOX treatment in Mrp1−/− cells could be due to decreased GSH efflux, increased GSH

biosynthesis, or increased/decreased recycling from GSSG. We therefore examined the mRNA and protein expression of GSH biosynthesis enzymes and GSH reductase (GR) (Figure 6A). DOX significantly increased mRNA and protein expression of GCLc and GCLm at 24 h in Mrp1−/− CM but only increased GCLc in WT CM. Similar results were observed in CF (Figure 6B). The DOX-induced increases in GCLc and GCLm expression in CM and CF were significantly greater in Mrp1−/− cells than WT cells, implying a greater adaptive response to oxidative stress. DOX had no effect on GR protein expression in either genotype (data not shown).

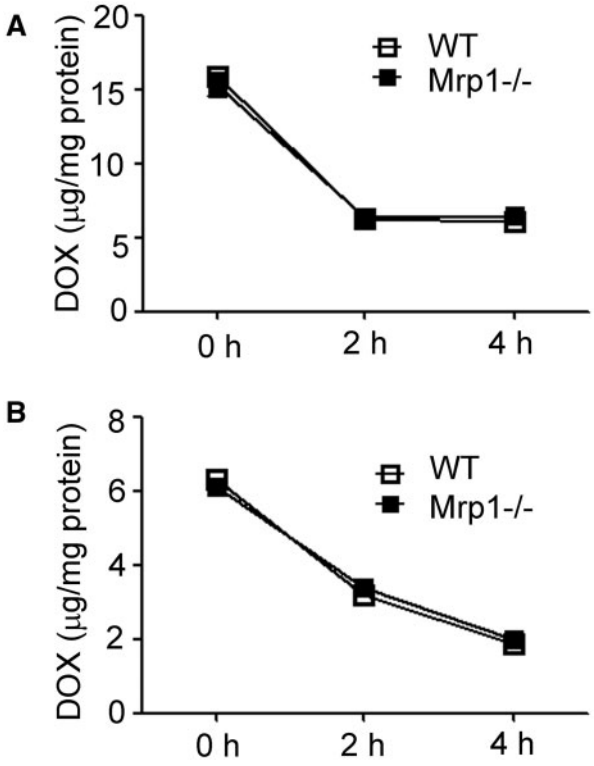

FIG. 3. Accumulation of DOX in WT and Mrp1−/− CM and CF. Cells were treated with 30 µM DOX for 1 h, cells washed 3 times with PBS and incubated with fresh DMEM medium for the indicated times and DOX fluorescence by spectrofluorometry. The value of DOX accumulation within the cells was calculated according to the standard curve. Each point represents the mean ± SD ($n = 3$).

Protein Expression of Antioxidant Enzymes

We next examined the expression of important antioxidant enzymes; DOX did not affect protein expression of catalase, Cu, ZnSOD, and MnSOD in either CM or CF of either genotype (data not shown). However, we unexpectedly found that mRNA and protein expression of SOD3 were significantly decreased in Mrp1−/− versus WT CM in saline-treated cells (64% ± 2% of WT mRNA, $P < .05$; 62% ± 8% of WT protein, $P < .05$) (Figure 7A). DOX treatment significantly decreased the expression of SOD3 in both WT and Mrp1−/− CM, such that SOD3 expression remained significantly lower in Mrp1−/− CM (46% ± 5% of WT mRNA, $P < .05$; 43% ± 12% of WT protein, $P < .05$). Decreased basal expression of SOD3 was not observed in CF (Figure 7B), indicating a cell-specific regulation of its expression and that CF are not a critical target. We also quantitated mRNA expression of glutathione peroxidase (Gpx), glutathione S-transferase (GST), NAD(P)H:quinone oxidoreductase 1 (NQO1), and heme oxygenase 1 (HO-1) and found that DOX increased mRNA expression of GPx1, GPx3, GSTM1, and GSTM2 in both WT and Mrp1−/− CM and CF, with GPx1 and GSTM1 mRNA increased slightly but significantly higher in DOX-treated Mrp1−/− versus WT CF (Supplementary Figure 2). Importantly, mRNA expression of NQO1 and HO-1 were significantly elevated in Mrp1−/− CM and CF compared with WT cells after DOX treatment (Supplementary Figure 3), indicative of activation of the antioxidant response.

DISCUSSION

This study is the first to show that loss of Mrp1 potentiates DOX-induced toxicity in CM and CF despite comparable levels of intracellular DOX between genotypes, and an increased intracellular concentration of GSH in Mrp1−/− cells. The data also

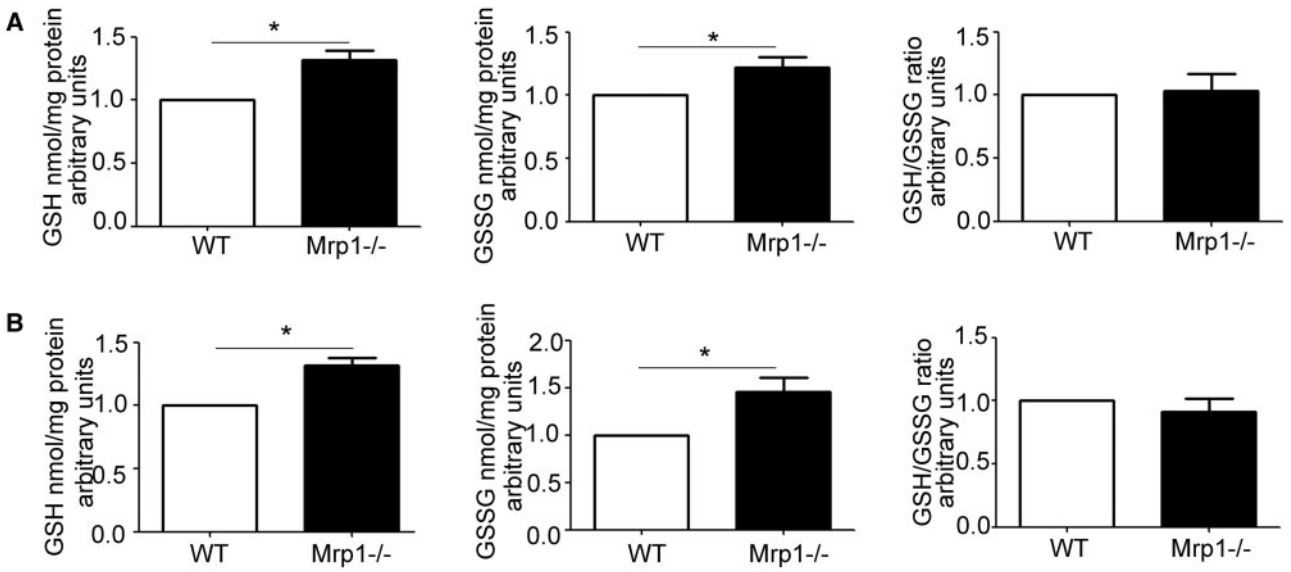

FIG. 4. Concentration of glutathione (GSH), glutathione disulfide (GSSG), and the GSH/GSSG ratio in untreated CM (A) and CF (B). GSH and GSSG were measured by HPLC. Each bar represents the mean ± SD ($n = 3$, *$P < .01$ by Welch's t test).

indicate a greater DOX-induced toxicity in CM versus CF, likely due to the higher concentrations of DOX in CM, attributable to the high number of mitochondria present in CM coupled with the high specific binding of DOX to mitochondrial cardiolipin (Varga *et al.*, 2015). Loss of Mrp1 in C57BL/6J mice potentiates nuclear damage in heart and induces significant cardiac dysfunction following acute (Deng *et al.*, 2015) and chronic (Zhang *et al.*, 2015) DOX treatment, respectively. Therefore, in the present studies, we investigated how Mrp1 affected DOX-induced toxicity in 2 critical cell types in the heart, CM, and CF.

Mrp1 was consistently expressed in cultured neonatal CM and CF from WT mice, and this expression was increased by DOX in a dose-dependent manner, with an apparent greater induction of Mrp1 protein in CM. More importantly, Mrp1−/− cells, especially Mrp1−/− CM, appeared more sensitive to DOX-induced cytotoxicity, showing decreased cell survival. Specifically, more apoptotic cell death in Mrp1−/− cells was demonstrated by higher caspase 3 and PARP cleavage, while more DNA damage was shown as higher γH2AX levels. Because CM and CF required different culture conditions and were examined at different times (CM require completion of experiments within 7 days, while CF require 2 passages to eliminate non-CF cells before experimentation), it was not possible to make a direct comparison regarding their relative sensitivity. Nevertheless, the greater sensitivity of CM to DOX was retained, and possibly enhanced in Mrp1−/− versus WT cells. The data demonstrating increased apoptosis in Mrp1−/− cells agree with findings in the *in vivo* Mrp1−/− mouse model, which showed increased DOX-induced nuclear injury detected by electron microscopy and cell apoptosis by the terminal deoxynucleotidyl transferase dUTP nick end labeling (TUNEL) assay in heart tissue (Deng *et al.*, 2015; Zhang *et al.*, 2015).

A key component of the cellular defense against oxidative injury is the intracellular redox buffer, with GSH and GSSG being the most abundant redox couple in the cell (Jones, 2008). A major determinant of cellular GSH homeostasis is GCL, which

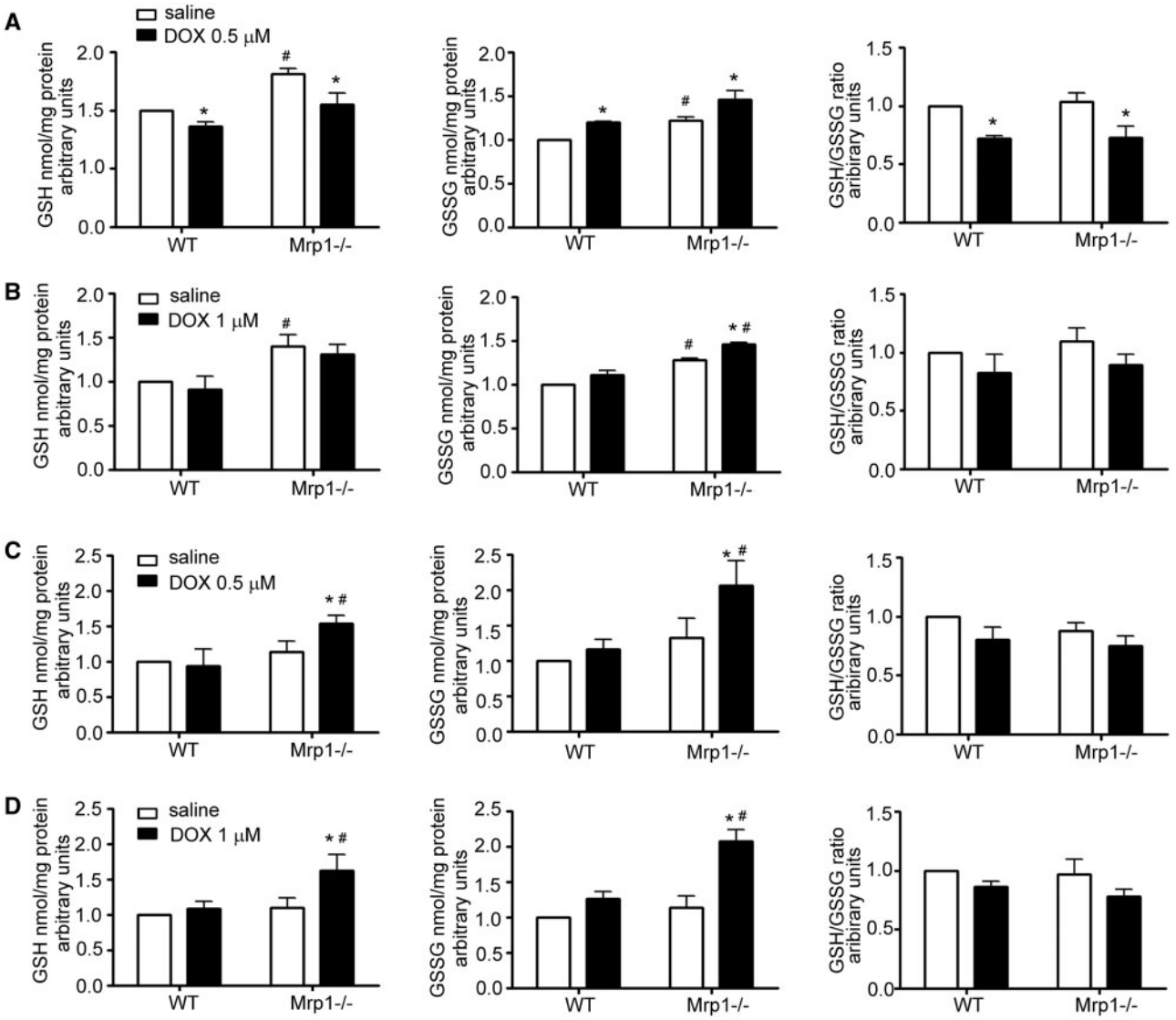

FIG. 5. Effects of DOX on the concentration of GSH, GSSG, and the GSH/GSSG ratio in CM and CF. CM (A) and CF (B) were treated with saline or DOX (CM, 0.5 μM; CF, 1 μM) for 15 min, and GSH and GSSG measured by HPLC. CM (C) and CF (D) were treated with saline or DOX (CM, 0.5 μM; CF, 1 μM) for 3 h, the medium removed and cells incubated in fresh medium for another 24 h, and GSH and GSSG measured by HPLC. Each bar represents the mean ± SD ($n = 3$; *$P < .05$ DOX vs saline of the same genotype; #$P < .05$ Mrp1−/− vs respective WT cells by Newman-Keuls multiple comparison test after 1-way ANOVA).

TABLE 2. The Redox Potential (*Eh*) of the GSH/GSSG Pool (15 min)

Cell	Mice	*Eh* of GSH/GSSG (mV) Ave ± SD	
		Treatment	
		saline	DOX
CM	WT	−237.7 ± 2.3	−231.4 ± 0.8*
	Mrp1−/−	−240.6 ± 1.6	−234.8 ± 2.3*
CF	WT	−236.5 ± 1.3	−230.0 ± 5.4
	Mrp1−/−	−239.4 ± 2.5	−235.4 ± 2.2

The redox potential (*Eh*) of the GSH/GSSG pool in CM and CF 15 min after saline or DOX. CM and CF were treated with saline or DOX (CM, 0.5 μM; CF, 1 μM) for 15 min. *Eh* is calculated by the Nernst equation, $Eh = Eo + (RT/nF)\ \ln([GSSG]/[GSH]^2)$. To estimate cellular concentrations, 1 mg of cell protein was assumed to be associated with 5 μl of cell volume (Mannery et al., 2010). R is the gas constant, T is temperature, *n* is the number of electrons transferred, F is the Faraday constant, and $Eo = -264$ mV at a pH of 7.4. Data are presented as mean ± SD ($n = 3$; *$P < .05$ DOX vs 0 min of the same genotype by Dunnett's posttest after 1-way ANOVA).

TABLE 3. The Redox Potential (*Eh*) of the GSH/GSSG Pool (24 h)

Cell	Mice	*Eh* of GSH/GSSG (mV) Ave ± SD	
		Treatment	
		Saline	DOX
CM	WT	−234.6 ± 1.6	−229.1 ± 7.0
	Mrp1−/−	−234.8 ± 2.7	−236.5 ± 1.2
CF	WT	−235.4 ± 3.0	−235.0 ± 2.1
	Mrp1−/−	−237.7 ± 1.0	−239.5 ± 5.1

The redox potential (*Eh*) of the GSH/GSSG pool in CM and CF 24 h after saline or DOX treatment. CM and CF were treated with saline or DOX (CM, 0.5 μM; CF, 1 μM) for 3 h, the medium removed and cells incubated in fresh medium for another 24 h. *Eh* is calculated by the Nernst equation, $Eh = Eo + (RT/nF)\ \ln([GSSG]/[GSH]^2)$ as described in Table 2. Data are presented as mean ± SD, $n = 3$.

catalyzes the rate-limiting step in *de novo* synthesis of GSH from glutamate and cysteine. GCL activity is regulated by (1) transcriptional activation following oxidative stress, (2) reversible formation of disulfide bonds between 2 subunits (GCLc and GCLm), and (3) feedback inhibition by GSH (Franklin *et al.*, 2009; Fraser *et al.*, 2003; Huang *et al.*, 1993; Richman *et al.*, 1975). The GSH concentration was higher in untreated Mrp1−/− versus WT cells (Figure 4), and in the absence of any differences in GCLc and GCLm expression (Figure 6), indicated that feedback inhibition of GCL was not sufficient to decrease the overall rate of GSH synthesis so as to return GSH to levels in WT cells. These data imply that loss of Mrp1-mediated GSH efflux is a major determinant of the intracellular GSH concentration. DOX further increased the concentration of GSH at 24 h in Mrp1−/− but not WT cells (Figure 5), consistent with the significantly increased expression of GCLc and GCLm in Mrp1−/− versus WT cells (Figure 6). GCLc and GCLm expression is regulated by the antioxidant response pathway at the transcriptional level following oxidative stress. Increased expression of NQO1 and HO-1, genes whose induction is also mediated by the antioxidant pathway, confirmed greater activation of the antioxidant response in DOX-treated Mrp1−/− versus WT cells, despite a higher intracellular concentration of GSH. It is important to note that the *Eh* for GSH/GSSG did not differ between WT and Mrp1−/− cells regardless of treatment conditions, and indicates that maintenance of the *Eh* is a critical endpoint for the cell. Nevertheless, despite a higher GSH concentration and comparable *Eh* for GSH/GSSG, Mrp1−/− cells were significantly more sensitive to DOX-induced toxicity.

The emerging concept of reductive stress may help explain why increased GSH does not rescue Mrp1−/− cells from DOX toxicity. Excessive amounts of reducing equivalents, in the forms of NAD(P)H and/or GSH, can result in cellular dysfunction and cardiac disease (Brewer *et al.*, 2012; Narasimhan *et al.*, 2015). Thus, overexpression of heat shock protein HSP2 leads to an increased GSH/GSSG ratio but results in cardiomyopathy (Zhang *et al.*, 2010). The human mutant αB-crystallin overexpression mouse model shows sustained activation of the Nrf2 signaling pathway, increases in GSH and the GSH/GSSG ratio, yet hypertrophic cardiomyopathy (Rajasekaran *et al.*, 2007, 2011), and a recent study indicates that GSH-induced reductive stress is causally linked to mitochondrial oxidation and cytotoxicity (Zhang *et al.*, 2012). In the present studies, Mrp1−/− cells had significantly higher GSH *and* GSSG concentrations in saline controls that were further increased by DOX treatment. The sustained activation of the antioxidant response and upregulation of GSH synthetic enzymes in DOX-treated Mrp1−/− cells is in contrast to the anticipated return to steady-state after the appropriate antioxidant cellular response observed in WT cells. It is possible that in DOX-treated Mrp1−/− cells, the abnormal redox signaling activation and compensatory responsiveness lead to cytotoxic consequences due to reductive stress. However, because the GSH/GSSG ratio was not different between genotypes, further studies, including measures of NADPH/NADP, a battery of antioxidant enzymes and oxidative stress markers, are needed to explore this hypothesis rigorously.

GSH depletion is a common feature of apoptosis induced by various stress conditions. GSH depletion could be mediated by its oxidation to GSSG, efflux of GSH via transporters or the loss of membrane integrity (Circu *et al.*, 2008; Franco *et al.*, 2007; Hammond *et al.*, 2004). Several studies have shown that prevention of GSH efflux can attenuate or prevent apoptosis (Circu *et al.*, 2009; Ghibelli *et al.*, 1998; He *et al.*, 2003). However, conflicting results exist regarding the identity of the specific transporter involved in GSH depletion, with several studies showing a role for MRP1 in GSH depletion (Hammond *et al.*, 2007; Laberge *et al.*, 2007; Mueller *et al.*, 2005; Sreekumar *et al.*, 2012), while others demonstrating that inhibition of MRP1-mediated transport accelerates apoptosis and GSH loss (Franco *et al.*, 2007, 2014). Discrepancies could be due to differences in cell types, culture conditions, MRP1 expression, duration of stress, the apoptotic stimulus, and GSH levels maintained during experimentation. In this study, in the absence of Mrp1-mediated GSH efflux, Mrp1−/− cells were significantly more sensitive to DOX-induced apoptosis, indicating that Mrp1-mediated GSH efflux is not essential and not the major determinant of DOX-induced apoptosis.

A novel and key finding is the significantly decreased expression of ECSOD/SOD3 in Mrp1−/− versus WT CM under basal conditions (saline treatment), and the further decrease following DOX treatment (Figure 7). Among the 3 SOD isoforms (Cu, ZnSOD, MnSOD2, and ECSOD), ECSOD is the sole enzyme located in the extracellular matrix catalyzing the dismutation of superoxide ($O_2^{\bullet -}$) to hydrogen peroxide (H_2O_2) and O_2 so as to maintain relatively low levels of $O_2^{\bullet -}$ in the extracellular environment. These low levels of $O_2^{\bullet -}$ are critical for minimizing formation of peroxynitrite-induced vascular injury in the presence of nitric oxide (NO) (Fukai *et al.*, 2002). Thus, overexpression of ECSOD in heart tissue or ECSOD administration attenuates oxidative stress, increases NO bioavailability in

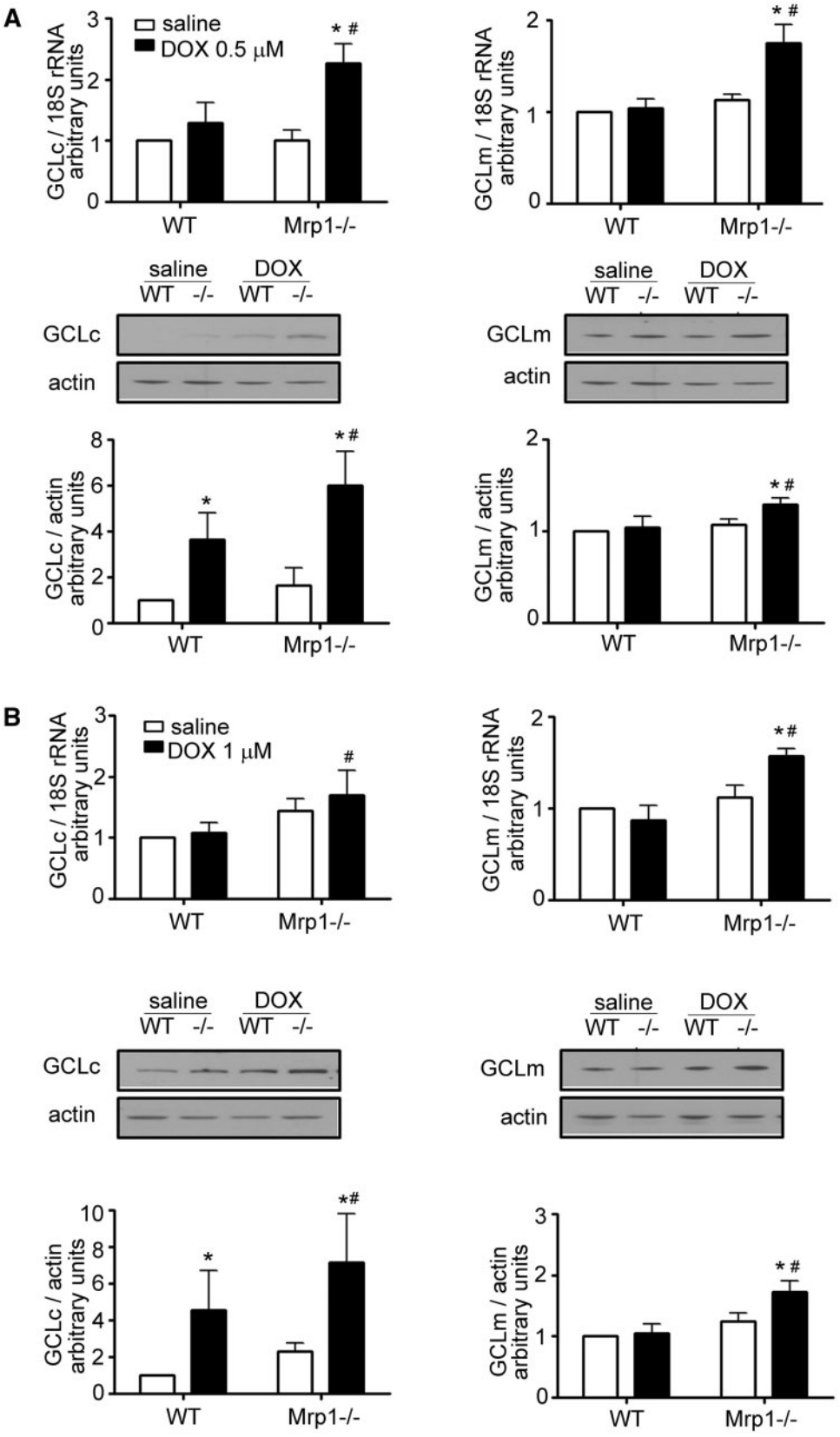

FIG. 6. Quantitative analysis of GCLc (glutamate-cysteine ligase, catalytic subunit) and GCLm (glutamate-cysteine ligase, regulatory subunit) in DOX-treated CM and CF. CM (A) and CF (B) were treated with saline or DOX (CM, 0.5 μM; CF, 1 μM) for 3 h, the medium removed and cells incubated in fresh medium for another 24 h. The immunoblots are representative of 1 of 3 independent experiments. Each bar represents the mean ± SD. (*$P < .05$ DOX vs saline of the same genotype; #$P < .05$ Mrp1−/− vs respective WT cells by Newman-Keuls multiple comparison test after 1-way ANOVA).

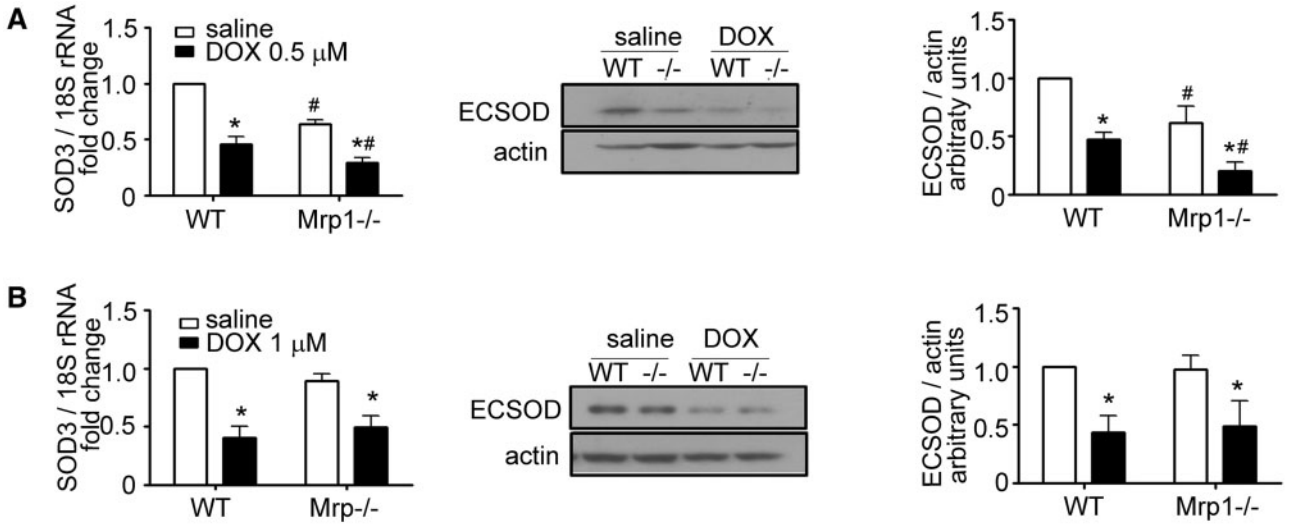

FIG. 7. Quantitative analysis of SOD3 mRNA and protein expression in DOX-treated CM and CF. CM (A) and CF (B) were treated with saline or DOX (CM, 0.5 μM; CF, 1 μM) for 3 h, the medium removed and cells incubated in fresh medium for another 24 h. The immunoblots are representative of 1 of 3 independent experiments. Each bar represents the mean ± SD. (*$P < .05$ DOX vs saline of the same genotype; #$P < .05$ Mrp1−/− vs respective WT cells by Newman-Keuls multiple comparison test after 1-way ANOVA).

response to ischemia/reperfusion and also mitigates tissue dysfunction in cardiovascular disease (Li *et al.*, 2001, 1998; Obal *et al.*, 2012; Wahlund *et al.*, 1992;). Importantly, DOX treatment of ECSOD null mice causes greater myocardial apoptosis and significantly more left ventricle fibrosis relative to WT mice (Kliment *et al.*, 2009), and suggests that the decreased ECSOD expression in Mrp1−/− CM contributes significantly to their greater sensitivity to DOX. Further, type II alveolar epithelial cells derived from Nrf2−/− mice show significantly higher SOD3 mRNA expression compared with WT cells, while GSH supplementation of these Nrf2−/− cells decreases SOD3 expression to that of WT cells (Reddy *et al.*, 2007). These data are consistent with modulation of the redox state by DOX and Mrp1, and the higher GSH concentration and decreased SOD3 expression observed in Mrp1−/− CM.

This differential ECSOD expression between genotype was not detected in CF (Figure 7). In further studies comparing WT CM versus CF, we noted that CF have much higher ECSOD expression than CM at both mRNA (approximately 3.4-fold) and protein (approximately 2.2-fold) levels (Supplementary Figure 4). Upon DOX treatment, ECSOD protein expression decreased in a dose-dependent manner in CM, while in CF, 0.5 μM DOX decreased while 3 μM DOX significantly increased ECSOD protein expression. The different basal levels of ECSOD expression coupled with a differential regulation of expression in CM and CF in response to DOX indicate that measurement of ECSOD expression in whole heart tissue can be misleading as it does not distinguish changes of ECSOD expression in these 2 different cell populations. How these sources of ECSOD coordinate with each other to minimize extracellular oxidative stress and contribute to DOX-induced pathological changes in heart will require more careful investigation.

In summary, the key finding of this *in vitro* study is that loss of Mrp1 potentiates DOX cytotoxicity in CM and CF, presenting as more severe apoptosis and DNA damage, consistent with *in vivo* findings of nuclear injury and apoptosis (Deng *et al.*, 2015; Zhang *et al.*, 2015), and confirming the cardiac protective function of Mrp1. Conservation of the GSH/GSSG redox couple in saline- and DOX-treated cells from both genotypes suggests that the changes in intracellular GSH and GSSG are not significant contributors to the increased susceptibility of Mrp1−/− cells to DOX. However, the loss of Mrp1-mediated efflux of GSH from cells almost certainly contributes to the decreased ability to scavenge $O_2^{\bullet -}$ in the extracellular environment, particularly of CM where expression of ECSOD is decreased, so that it may be the increased *extracellular* oxidative stress that mediates greater susceptibility of Mrp1−/− cells, particularly CM, to DOX-induced cardiotoxicity. Alternatively, the loss of Mrp1-mediated efflux of additional important substrates, including signaling molecules, such as nitrolinoleic acid (Alexander *et al.*, 2006) or potentially cytotoxic dinitrosyl-diglutathionyl iron complexes (Lok *et al.*, 2012), may make Mrp1−/− cells vulnerable to greater DOX-induced cytotoxicity. Clearly, additional studies are needed to understand the complex mechanisms by which Mrp1 protects the heart. Lastly, due to its role in multidrug resistance development in cancer cells, MRP1 is considered as a diagnostic marker and a therapeutic target to increase the efficacy of a variety of chemotherapy drugs, including anthracyclines (Schaich *et al.*, 2005; Faggad *et al.*, 2009). Here, our studies provide critical information regarding the potential adverse sequelae of introduction of MRP1 inhibitors as adjuncts to clinical chemotherapy of multidrug resistant tumors.

SUPPLEMENTARY DATA

Supplementary data are available online athttp://toxsci.oxfordjournals.org/.

FUNDING

This work was supported by the National Cancer Institute of the National Institutes of Health (CA139844); W.Z. was supported by an American Heart Association Predoctoral Fellowship (grant number 17060037).

ACKNOWLEDGMENTS

The authors thank the Biostatistics and Bioinformatics Shared Resource and the Redox Metabolism Shared Resource of the Markey Cancer Center (P30 CA177558) for

their support. They also thank Dr Jonathon Satin, University of Kentucky, Lexington, KY for the generous help with neonatal mouse cardiomyocyte isolation methods. They thank Dr Ladislav Dory, University of North Texas, Denton, TX for a generous gift of rabbit anti-ECSOD pAb.

REFERENCES

Alexander, R. L., Bates, D. J., Wright, M. W., King, S. B., and Morrow, C. S. (2006). Modulation of nitrated lipid signaling by multidrug resistance protein 1 (MRP1): Glutathione conjugation and MRP1-mediated efflux inhibit nitrolinoleic acid-induced, PPARgamma-dependent transcription activation. *Biochemistry* **45**, 7889–7896.

Barth, E., Stämmler, G., Speiser, B., and Schaper, J. (1992). Ultrastructural quantitation of mitochondria and myfilaments in cardiac muscle from 10 different animal species including man. *J. Mol. Cell Cardiol.* **24**, 669–681.

Brewer, A. C., Mustafi, S. B., Murray, T. V., Rajasekaran, N. S., and Benjamin, I. J. (2012). Reductive stress linked to small HSPs, G6PD, and Nrf2 pathways in heart disease. *Antioxid. Redox Signal.* **18**, 1114–1127.

Camelliti, P., Borg, T. K., and Kohl, P. (2005). Structural and functional characterisation of cardiac fibroblasts. *Cardiovasc. Res.* **65**, 40–51.

Chen, Y., Daosukho, C., Opii, W. O., Turner, D. M., Pierce, W. M., Klein, J. B., Vore, M., Butterfield, D. A., and St Clair, D. K. (2006). Redox proteomic identification of oxidized cardiac proteins in adriamycin-treated mice. *Free Radic. Biol. Med.* **41**, 1470–1477.

Circu, M. L., and Aw, T. Y. (2008). Glutathione and apoptosis. *Free Radic. Res.* **42**, 689–706.

Circu, M. L., Stringer, S., Rhoads, C. A., Moyer, M. P., and Aw, T. Y. (2009). The role of GSH efflux in staurosporine-induced apoptosis in colonic epithelial cells. *Biochem. Pharmacol.* **77**, 76–85.

Cole, S. P. (2014a). Multidrug resistance protein 1 (MRP1, ABCC1): A 'multitasking' ABC transporter. *J. Biol. Chem.* **289**, 30880–30888.

Cole, S. P. (2014b). Targeting the multidrug resistance protein (MRP1, ABCC1): Past, present and future. *Annu. Rev. Pharmacol. Toxicol.* **54**, 95–117.

Cole, S. P., and Deeley, R. G. (1998). Multidrug resistance mediated by the ATP-binding cassette transporter protein MRP. *Bioessays* **20**, 931–940.

Deng, J., Coy, D. J., Zhang, W., Sunkara, M., Morris, A., Wang, C., Chaiswing, L., St Clair, D. K., Vore, M., and Jungsuwadee, P. (2015). Elevated glutathione is not sufficient to protect against doxorubicin-induced nuclear damage in heart in multidrug resistance associated protein 1 (Mrp1/Abcc1) null mice. *J.Pharm. Exp. Ther.* **355**, 272–279.

Doyle, J. J., Neugut, A. I., Jacobson, J. S., Grann, V. R., and Hershman, D. L. (2005). Chemotherapy and cardiotoxicity in older breast cancer patients: A population-based study. *J. Clin. Oncol.* **23**, 8597–8605.

Faggad, A., Darb-Esfahani, S., Wirtz, R., Sinn, B., Sehouli, J., Könsgen, D., Lage, H., Noske, A., Weichert, W., Buckendahl, A. C., *et al.* (2009). Expression of multidrug resistance-associated protein 1 in invasive ovarian carcinoma: Implication for prognosis. *Histopathology* **54**, 657–666.

Flens, M., Zaman, G., van der Valk, P., Izquierdo, M., Schroeijers, A., Scheffer, G., van der Groep, P., de Haas, M., Meijer, C., and Scheper, R. (1996). Tissue distribution of the multidrug resistance protein. *Am. J. Pathol.* **148**, 1237–1247.

Franco, R., Bortner, C. D., Schmitz, I., and Cidlowski, J. A. (2014). Glutathione depletion regulates both extrinsic and intrinsic apoptotic signaling cascades independent from multidrug resistance protein 1. *Apoptosis* **19**, 117–134.

Franco, R., Panayiotidis, M. I., and Cidlowski, J. A. (2007). Glutathione depletion is necessary for apoptosis in lymphoid cells independent of reactive oxygen species formation. *J. Biol. Chem.* **282**, 30452–30465.

Franklin, C. C., Backos, D. S., Mohar, I., White, C. C., Forman, H. J., and Kavanagh, T. J. (2009). Structure, function, and post-translational regulation of the catalytic and modifier subunits of glutamate cysteine ligase. *Mol. Aspects Med.* **30**, 86–98.

Fraser, J. A., Kansagra, P., Kotecki, C., Saunders, R. D., and McLellan, L. I. (2003). The modifier subunit of Drosophila glutamate-cysteine ligase regulates catalytic activity by covalent and noncovalent interactions and influences glutathione homeostasis in vivo. *J. Biol. Chem.* **278**, 46369–46377.

Fu, Z., Guo, J., Jing, L., Li, R., Zhang, T., and Peng, S. (2010). Enhanced toxicity and ROS generation by doxorubicin in primary cultures of cardiomyocytes from neonatal metallothionein-I/II null mice. *Toxicol. In Vitro* **24**, 1584–1591.

Fukai, T., Folz, R. J., Landmesser, U., and Harrison, D. G. (2002). Extracellular superoxide dismutase and cardiovascular disease. *Cardiovasc. Res.* **55**, 239–249.

Ghibelli, L., Fanelli, C., Rotilio, G., Lafavia, E., Coppola, S., Colussi, C., Civitareale, P., and Ciriolo, M. R. (1998). Rescue of cells from apoptosis by inhibition of active GSH extrusion. *FASEB J.* **12**, 479–486.

Hammond, C. L., Madejczyk, M. S., and Ballatori, N. (2004). Activation of plasma membrane reduced glutathione transport in death receptor apoptosis of HepG2 cells. *Toxicol. Appl. Pharmacol.* **195**, 12–22.

Hammond, C. L., Marchan, R., Krance, S. M., and Ballatori, N. (2007). Glutathione export during apoptosis requires functional multidrug resistance-associated proteins. *J. Biol. Chem.* **282**, 14337–14347.

He, Y. Y., Huang, J. L., Ramirez, D. C., and Chignell, C. F. (2003). Role of reduced glutathione efflux in apoptosis of immortalized human keratinocytes induced by UVA. *J. Biol. Chem.* **278**, 8058–8064.

Huang, C. S., Chang, L. S., Anderson, M. E., and Meister, A. (1993). Catalytic and regulatory properties of the heavy subunit of rat kidney gamma-glutamylcysteine synthetase. *J. Biol. Chem.* **268**, 19675–19680.

Jones, D. P. (2008). Radical-free biology of oxidative stress. *Am. J. Physiol. Cell Physiol.* **295**, C849–C868.

Kamkin, A., Kiseleva, I., Lozinsky, I., and Scholz, H. (2005). Electrical interaction of mechanosensitive fibroblasts and myocytes in the heart. *Basic Res. Cardiol.* **100**, 337–345.

Kliment, C. R., Suliman, H. B., Tobolewski, J. M., Reynolds, C. M., Day, B. J., Zhu, X., McTiernan, C. F., McGaffin, K. R., Piantadosi, C. A., and Oury, T. D. (2009). Extracellular superoxide dismutase regulates cardiac function and fibrosis. *J. Mol. Cell. Cardiol.* **47**, 730–742.

Krohn, M., Lange, C., Hofrichter, J., Scheffler, K., Stenzel, J., Steffen, J., Schumacher, T., Bruning, T., Plath, A. S., Alfen, F., *et al.* (2011). Cerebral amyloid-beta proteostasis is regulated by the membrane transport protein ABCC1 in mice. *J. Clin. Invest.* **121**, 3924–3931.

Laberge, R. M., Karwatsky, J., Lincoln, M. C., Leimanis, M. L., and Georges, E. (2007). Modulation of GSH levels in ABCC1

expressing tumor cells triggers apoptosis through oxidative stress. *Biochem. Pharmacol.* **73**, 1727–1737.

Leslie, E. M., Ito, K., Upadhyaya, P., Hecht, S. S., Deeley, R. G., and Cole, S. P. (2001). Transport of the β-O-glucuronide conjugate of the tobacco-specific carcinogen 4-(methylnitrosamino)-1-(3- pyridyl)-1-butanol (NNAL) by the multidrug resistance protein 1 (MRP1). Requirement for glutathione or a non-sulfur-containing analog. *J. Biol. Chem.* **276**, 27846–27854.

Li, Q., Bolli, R., Qiu, Y., Tang, X. L., Guo, Y., and French, B. A. (2001). Gene therapy with extracellular superoxide dismutase protects conscious rabbits against myocardial infarction. *Circulation* **103**, 1893–1898.

Li, Q., Bolli, R., Qiu, Y., Tang, X. L., Murphree, S. S., and French, B. A. (1998). Gene therapy with extracellular superoxide dismutase attenuates myocardial stunning in conscious rabbits. *Circulation* **98**, 1438–1448.

Li, Q., Kato, Y., Sai, Y., Imai, T., and Tsuji, A. (2005). Multidrug resistance-associated protein 1 functions as an efflux pump of xenobiotics in the skin. *Pharm. Res.* **22**, 842–846.

Lok, H. C., Suryo Rahmanto, Y., Hawkins, C. L., Kalinowsky, D. S., Morrow, C. S., Townsend, A. J., Ponka, P., and Richardson, D. R. (2012). Nitric oxide storage and transport in cells are mediated by glutathione S-transferase P1-1 and multidrug resistance protein 1 via dinitrosyl iron complexes. *J. Biol. Chem.* **287**, 607–618.

Lorico, A., Rappa, G., Finch, R. A., Yang, D., Flavell, R. A., and Sartorelli, A. C. (1997). Disruption of the murine MRP (multidrug resistance protein) gene leads to increased sensitivity to etoposide (VP-16) and increased levels of glutathione. *Cancer Res.* **57**, 5238–5242.

Mannery, Y. O., Ziegler, T. R., Hao, L., Shyntum, Y., and Jones, D. P. (2010). Characterization of apical and basal thiol-disulfide redox regulation in human colonic epithelial cells. *Am. J. Physiol. Gastrointest. Liver Physiol.* **299**, G523–G530.

Mueller, C. F., Widder, J. D., McNally, J. S., McCann, L., Jones, D. P., and Harrison, D. G. (2005). The role of the multidrug resistance protein-1 in modulation of endothelial cell oxidative stress. *Circ. Res.* **97**, 637–644.

Narasimhan, M., and Rajasekaran, N. S. (2015). Reductive potential–A savior turns stressor in protein aggregation cardiomyopathy. *Biochim. Biophys. Acta* **1852**, 53–60.

Nies, A. T., Jedlitschky, G., Konig, J., Herold-Mende, C., Steiner, H. H., Schmitt, H.-P., and Keppler, D. (2004). Expression and immunolocalization of the multidrug resistance proteins, MRP1-MRP6 (ABCC1-ABCC6), in human brain. *Neuroscience* **129**, 349–360.

Obal, D., Dai, S., Keith, R., Dimova, N., Kingery, J., Zheng, Y. T., Zweier, J., Velayutham, M., Prabhu, S. D., Li, Q., *et al.* (2012). Cardiomyocyte-restricted overexpression of extracellular superoxide dismutase increases nitric oxide bioavailability and reduces infarct size after ischemia/reperfusion. *Basic Res. Cardiol.* **107**, 305.

Octavia, Y., Tocchetti, C. G., Gabrielson, K. L., Janssens, S., Crijns, H. J., and Moens, A. L. (2012). Doxorubicin-induced cardiomyopathy: From molecular mechanisms to therapeutic strategies. *J. Mol. Cell. Cardiol.* **52**, 1213–1225.

Rajasekaran, N. S., Connell, P., Christians, E. S., Yan, L. J., Taylor, R. P., Orosz, A., Zhang, X. Q., Stevenson, T. J., Peshock, R. M., Leopold, J. A., *et al.* (2007). Human alpha B-crystallin mutation causes oxido-reductive stress and protein aggregation cardiomyopathy in mice. *Cell* **130**, 427–439.

Rajasekaran, N. S., Varadharaj, S., Khanderao, G. D., Davidson, C. J., Kannan, S., Firpo, M. A., Zweier, J. L., and Benjamin, I. J. (2011). Sustained activation of nuclear erythroid 2-related factor 2/antioxidant response element signaling promotes reductive stress in the human mutant protein aggregation cardiomyopathy in mice. *Antioxid. Redox Signal.* **14**, 957–971.

Reddy, N. M., Kleeberger, S. R., Yamamoto, M., Kensler, T. W., Scollick, C., Biswal, S., and Reddy, S. P. (2007). Genetic dissection of the Nrf2-dependent redox signaling-regulated transcriptional programs of cell proliferation and cytoprotection. *Physiol. Genomics* **32**, 74–81.

Richman, P. G., and Meister, A. (1975). Regulation of gamma-glutamyl-cysteine synthetase by nonallosteric feedback inhibition by glutathione. *J. Biol. Chem.* **250**, 1422–1426.

Schaich, M., Soucek, S., Thiede, C., Ehninger, G., Illmer, T., and AML96 Study Group, S. H. G. (2005). MDR1 and MRP1 gene expression are independent predictors for treatment outcome in adult acute myeloid leukaemia. *Br. J. Haematol.* **128**, 324–332.

Semsei, A. F., Erdelyi, D. J., Ungvari, I., Csagoly, E., Hegyi, M. Z., and Kiszel, P. S. (2012). ABCC1 polymorphisms in anthracycline-induced cardiotoxicity in childhood acute lymphoblastic leukaemia. *Cell Biol. Int.* **36**, 79–86.

Shi, Q., Liu, X., Bai, Y., Cui, C., Li, J., Li, Y., Hu, S., and Wei, Y. (2011). In vitro effects of pirfenidone on cardiac fibroblasts: Proliferation, myofibroblast differentiation, migration and cytokine secretion. *PLoS One* **6**, e28134.

Souders, C. A., Bowers, S. L., and Baudino, T. A. (2009). Cardiac fibroblast: The renaissance cell. *Circ. Res.* **105**, 1164–1176.

Sreekumar, P. G., Spee, C., Ryan, S. J., Cole, S. P., Kannan, R., and Hinton, D. R. (2012). Mechanism of RPE cell death in α-crystallin deficient mice: A novel and critical role for MRP1-mediated GSH efflux. *PLoS One* **7**, e33420.

Stride, B. D., Grant, C. E., Loe, D. W., Hipfner, D. R., Cole, S. P., and Deeley, R. G. (1997). Pharmacological characterization of the murine and human orthologs of multidrug-resistance protein in transfected human embryonic kidney cells. *Mol. Pharmacol.* **52**, 344–353.

Varga, Z. V., Ferdinandy, P., Liaudet, L., and Pacher, P. (2015). Drug-induced mitochondrial dysfunction and cardiotoxicity. *Am. J. Physiol. Heart Circ. Physiol.* **309**, H1453–H1467.

Visscher, H., Ross, C. J., Rassekh, S. R., Barhdadi, A., Dubé, M. P., and Al-Saloos, H. (2012). Pharmacogenomic prediction of anthracycline-induced cardiotoxicity in children. *J. Clin. Oncol.* **30**, 1422–1428.

Wahlund, G., Marklund, S. L., and Sjoquist, P. O. (1992). dismutase type C (EC-SOD C) reduces myocardial damage in rats subjected to coronary occlusion and 24 hours of reperfusion. *Free Radic. Res. Commun.* **17**, 41–47.

Wijnholds, J., Evers, R., van Leusden, M. R., Mol, C. A., Zaman, G. J., Mayer, U., Beijnen, J. H., van der Valk, M., Krimpenfort, P., and Borst, P. (1997). Increased sensitivity to anticancer drugs and decreased inflammatory response in mice lacking the multidrug resistance-associated protein. *Nat. Med.* **3**, 1275–1379.

Wojnowski, L., Kulle, B., Schirmer, M., Schlüter, G., Schmidt, A., and Rosenberger, A. (2005). NAD(P)H oxidase and multidrug resistance protein genetic polymorphisms are associated with doxorubicin-induced cardiotoxicity. *Circulation* **112**, 3754–3762.

Yen, H. C., Oberley, T. D., Vichitbandha, S., Ho, Y. S., and St Clair, D. K. (1996). The protective role of manganese superoxide dismutase against adriamycin-induced acute cardiac toxicity in transgenic mice. *J. Clin. Invest.* **98**, 1253–1260.

Yin, G., Hassan, F., Haroun, A. R., Murphy, L. L., Crotti, L., Schwartz, P. J., George, A. L., and Satin, J. (2014). Arrhythmogenic calmodulin mutations disrupt intracellular

cardiomyocyte Ca^{2+} regulation by distinct mechanisms. *J. Am. Heart Assoc.* **3**, e000996.

Zhang, H., Limphong, P., Pieper, J., Liu, Q., Rodesch, C. K., Christians, E., and Benjamin, I. J. (2012). Glutathione-dependent reductive stress triggers mitochondrial oxidation and cytotoxicity. *FASEB J.* **26**, 1442–1451.

Zhang, W., Deng, J., Coy, D. J., Sunkara, M., Morris, A., Wang, C., St Clair, D. K., and Vore, M. (2015). Loss of Abcc1 (Mrp1) potentiates chronic doxorubicin-induced cardiac dysfunction in mice. *J. Pharmacol. Exp. Ther.* **355**, 280–287.

Zhang, X., Min, X., Li, C., Benjamin, I. J., Qian, B., Zhang, X., Ding, Z., Gao, X., Yao, Y., Ma, Y., *et al.* (2010). Involvement of reductive stress in the cardiomyopathy in transgenic mice with cardiac-specific overexpression of heat shock protein 27. *Hypertension* **55**, 1412–1417.

Zhang, Y. W., Shi, J., Li, Y. J., and Wei, L. (2009). Cardiomyocyte death in doxorubicin-induced cardiotoxicity. *Arch. Immunol. Ther. Exp.* **57**, 435–445.